ACI STRUCTURAL JOURNAL TECHNICAL PAPER

Title no. 107-S11

Evaluation of Steel Fiber Reinforcement for Punching Shear Resistance in Slab-Column Connections—Part I: Monotonically Increased Load

by Min-Yuan Cheng and Gustavo J. Parra-Montesinos

Results from an experimental investigation aimed at evaluating the effectiveness of steel fiber reinforcement for increasing punching shear strength and ductility in slabs subjected to monotonically increased concentrated load are presented. Ten slab-column connections were tested to failure. The main test parameters evaluated were: 1) fiber geometry (hooked or twisted), 2) fiber strength (1100, 1800, or 2300 MPa [160, 260, or 334 ksi]), 3) fiber volume fraction (1% or 1.5%), and 4) slab tension reinforcement ratio (0.56% or 0.83% in each principal direction). Out of the fiber-reinforced concretes (or mortar) evaluated, those reinforced with a 1.5% volume fraction of either regular strength (1100 MPa [160 ksi]) or high-strength (2300 MPa [334 ksi]) hooked steel fibers led to the best performance in terms of punching shear strength and deformation capacity. These two fiber-reinforced concretes (FRCs) were therefore selected for further evaluation in connections subjected to lateral displacement reversals, as described in the companion paper.

Keywords: fiber reinforcement; punching sheer; steel.

INTRODUCTION

Slab-column or flat plate frame systems offer several construction and architectural advantages, which make them a popular choice in reinforced concrete (RC) construction. Because the slab is supported directly by columns, formwork is substantially simpler and greater clear story heights can be achieved compared to beam-column frame construction, leading to substantial savings in construction costs. Having the slab supported directly by columns, however, makes the connections susceptible to punching shear failures, which could lead to substantial floor damage or even structural collapse.

Increasing the slab thickness or using drop panels or column capitals to increase connection shear capacity is often not an economical and/or practical option. Increasing slab thickness results in a cost and weight increase. On the other hand, changes in slab cross section and formwork when using drop panels or column capitals take away some of the major advantages of flat plate frame systems over beam-column frames, that is, uniformity in floor bottom surface and increased clear story heights. Therefore, methods to increase punching shear resistance without modifying the slab thickness are often preferred.

Several reinforcement alternatives for increasing punching shear resistance of slab-column connections, including bent-up bars (Hawkins et al. 1974; Islam and Park 1976), closed stirrups (Islam and Park 1976), shearheads (Corley and Hawkins 1968), and shear studs (Dilger and Ghali 1981), have been evaluated in the past five decades. The use of steel fiber reinforcement for punching shear resistance of slabs subjected to gravity-type loading has also been extensively investigated (for example, Swamy and Ali 1982; Shaaban and Gesund 1994; Alexander and Simmonds 1992; Harajli et al. 1995; McHarg et al. 2000; Naaman et al. 2007). Steel fibers have been experimentally shown to increase punching shear resistance and ductility. In some cases (Swamy and Ali 1982; Harajli et al. 1995), the use of fiber reinforcement has been claimed to lead to an enlargement of the punching shear surface.

Contrary to most previous research works on fiber-reinforced concrete (FRC) slab-column connections, the ultimate goal of this research was to evaluate the use of fiber reinforcement in connections subjected to large displacement reversals, such as those induced by earthquakes. As a first step toward this goal, however, an evaluation of the ability of various fiber-reinforced cement-based materials to increase punching shear strength and deformation capacity of slab-column connections subjected to monotonically increased concentrated load was conducted. This would allow the selection of the materials that led to the best performance to be further investigated under lateral displacement reversals.

Results from the tests of slabs subjected to monotonically increased concentrated load are presented in this paper, while the results from an investigation on the behavior of FRC slab-column connections under lateral displacement reversals are presented in the companion paper (Cheng and Parra-Montesinos 2010).

RESEARCH SIGNIFICANCE

New information about the behavior of steel FRC slab-column connections is presented. In particular, new data are provided on punching shear strength, rotation capacity, and the relationship between the two in FRC slab-column connections with various fiber types, fiber contents, and flexural reinforcement ratios.

RESEARCH DESCRIPTION

The research presented herein and in the companion paper (Cheng and Parra-Montesinos 2010) can be divided into two phases. In the first phase, which is the focus of this paper, a series of slabs was tested under monotonically increased concentrated load. Four different types of FRCs (or fiber-reinforced mortar) and two slab tensile reinforcement ratios were evaluated. This testing phase served two purposes: 1) to select the FRC materials with the best potential

ACI Structural Journal, V. 107, No. 1, January-February 2010.
MS No. S-2009-038.R1 received February 11, 2009, and reviewed under Institute publication policies. Pertinent discussion including author's closure, if any, will be published in the November-December 2010 *ACI Structural Journal* if the discussion is received by July 1, 2010.

Min-Yuan Cheng *is a Structural Engineer at Cary Kopzcynski and Company, Bellevue, WA. He received his BS in marine engineering from National Sun-Yat-Sen University, Taiwan; his MS in civil engineering from National Cheng Kung University, Tainan City, Taiwan; and his PhD in civil engineering from the University of Michigan, Ann Arbor, MI.*

ACI member **Gustavo J. Parra-Montesinos** *is an Associate Professor at the University of Michigan. He is Secretary of ACI Committee 335, Composite and Hybrid Structures, and a member of the ACI Publications Committee; ACI Committees 318, Structural Concrete Building Code; and Joint ACI-ASCE Committee 352, Joints and Connections in Monolithic Concrete Structures. His research interests include the behavior and design of reinforced concrete, fiber-reinforced concrete, and composite steel-concrete structures.*

for use in slab-column connections subjected to earthquake-induced deformations, and 2) to estimate an upper limit for slab punching shear strength that could be later compared with the strength of slab-column connections subjected to combined gravity load and lateral displacement reversals.

The second research phase, described in the companion paper (Cheng and Parra-Montesinos 2010), consisted of the evaluation of the behavior of steel FRC slab-column connections under combined gravity load and lateral displacement reversals. Detailed information about the entire research program can be found elsewhere (Cheng and Parra-Montesinos 2009).

Slab specimens and testing method

The main parameters evaluated were steel fiber geometry, fiber steel strength, fiber content, and flexural reinforcement ratio. Ten specimens, which represented isolated interior slab-column connections, were tested under monotonically increased concentrated load. The slab dimensions were the same for all ten specimens, 1.5 x 1.5 x 0.15 m (60 x 60 x 6 in.), with a 15 cm (6 in.) square column stub at the center of the slab for load application. Figure 1 shows a sketch of the slab specimens and test setup. The slab specimens were tested upside down, which meant that tension in the connection region was induced at the bottom of the slab, as opposed to the top, as is the case in connections of flat plate construction subjected to gravity loads.

A vertically oriented hydraulic actuator connected to a steel reaction frame was used for application of the load to the slab specimens, as shown in Fig. 1. The test specimens were supported along their perimeter on a 13 mm (0.5 in.) thick neoprene pad placed on top of a steel tube with a cross section of 76 x 127 x 6 mm (3 x 5 x 0.25 in.) to simulate a simply supported boundary condition. Under this test configuration, the corners of the slab were free to lift. The load at the column stub was applied through a monotonically increased displacement at a rate of 3.8 mm/min.

For each type of fiber-reinforced cement-based material (or plain concrete), two slabs were tested. One slab specimen contained flexural reinforcement at a 0.83% ratio in each principal direction, whereas the reinforcement ratio in the other specimen was 0.56%. Only bottom reinforcement was provided. Figure 2 shows the reinforcement layout for each reinforcement ratio. The same reinforcing bar size (No. 13M, that is, 13 mm diameter) was used in all test specimens and, thus, only the bar spacing was varied between the two specimens tested for each material evaluated. The bar spacing was either 102 mm (4 in.) (Specimens S1, S3, S5, S7, and S9) or 152 mm (6 in.) (Specimens S2, S4, S6, S8, and S10). All reinforcing bars were made of Grade 420M steel. The slab effective depth d, taken as the average value for both reinforcement directions, was equal to 127 mm (5 in.).

The main difference between each fiber-reinforced material was in the fiber type and volume content and whether a

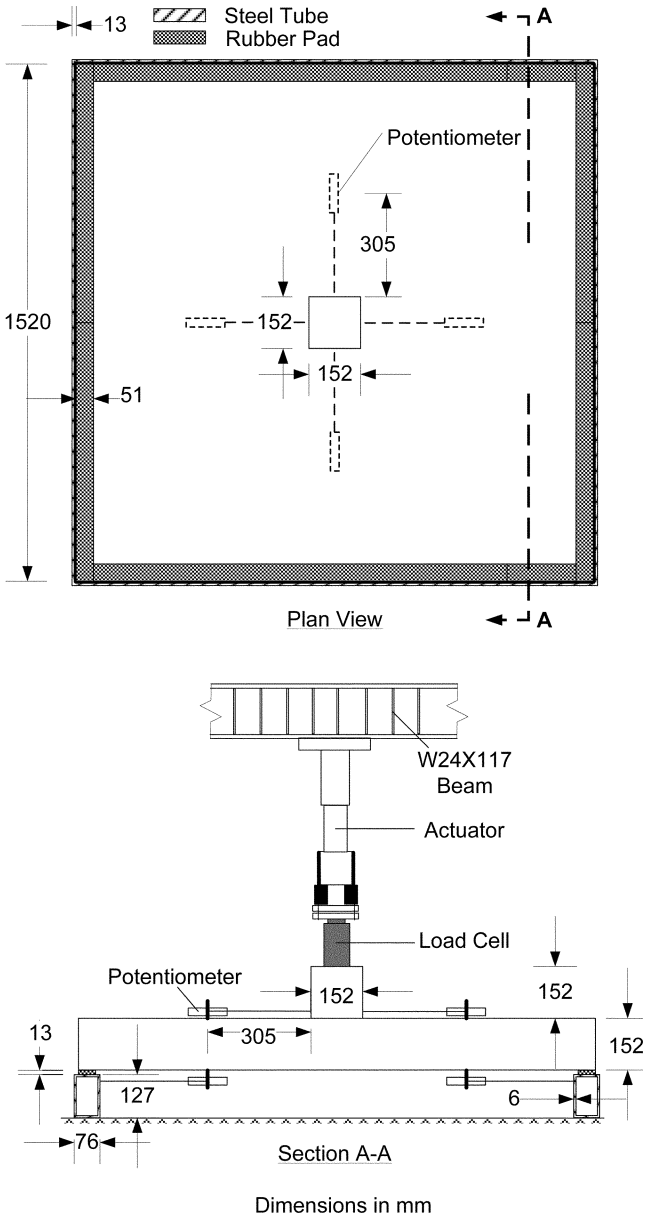

Fig. 1—Test configuration.

concrete or mortar mixture was used. Table 1 summarizes the main features of each specimen. It is worth mentioning that FRC in specimen pairs S5 and S6, and S9 and S10 was only used within a 762 mm (30 in.) square portion at the center of the slab (two slab thicknesses from each column stub face), the remaining of the slab being constructed with regular concrete.

Strains in the slab reinforcement were measured through strain gauges located at 0.5d and 1.5d away from the column stub faces. The location of each strain gauge is shown in Fig. 2. Slab rotations, on the other hand, were measured over a distance of 305 mm (12 in.) from each column stub face (twice the slab thickness) through four pairs of linear potentiometers, as shown in Fig. 1. The tests were terminated when a significant loss of load-carrying capacity was observed.

MATERIAL PROPERTIES

Concrete

All concrete mixtures were designed for a 28-day compressive strength of approximately 35 MPa (5000 psi).

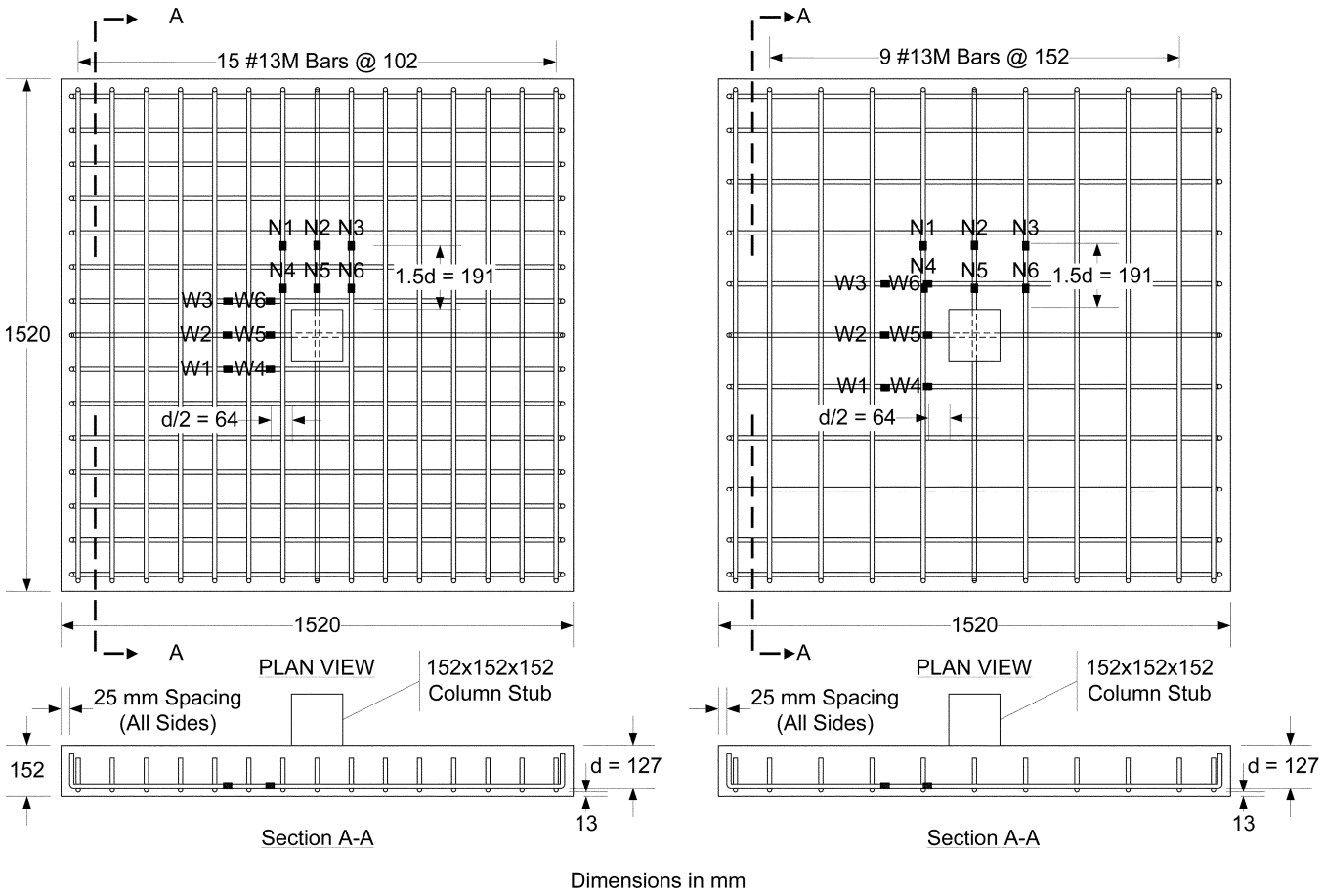

Fig. 2—Reinforcement layout and strain gauge location.

Table 1—Material and fiber properties

Specimen	Concrete		Steel fibers			Steel bars		
	Material	Strength, MPa	Fiber type (V_f)	L_f (d_f), mm	f_u, MPa	ρ, %	f_y, MPa	f_u, MPa
S1	Plain	47.7	—	—	—	0.83	471	697
S2						0.56		
S3	FRC	25.4	Hooked (1%)	30 (0.55)	1100	0.83	455	670
S4						0.56		
S5	FRM*	59.3	Twisted (1.5%)	35 (0.5)†	1800	0.83	471	689
	Plain	45.7	—	—	—			
S6	FRM*	57.9	Twisted (1.5%)	35 (0.5)†	1800	0.56		
	Plain	35.0	—	—	—			
S7	FRC	31.0	Hooked (1.5%)	30 (0.55)	1100	0.83	449	681
S8						0.56		
S9	FRC*	46.1	Hooked (1.5%)	30 (0.38)	2300	0.83		
	Plain	40.7	—	—	—			
S10	FRC*	59.1	Hooked (1.5%)	30 (0.38)	2300	0.56		
	Plain	50.6	—	—	—			

*Only in central 76 x 76 cm (30 x 30 in.) region of slab.
†Equivalent diameter.
Notes: FRC is fiber-reinforced concrete; FRM is fiber-reinforced mortar; V_f is fiber volume fraction; L_f is fiber length; d_f is fiber diameter; ρ is reinforcement ratio in each direction (0.83%: No. 13M at 10 cm [4 in.]; 0.56%: No. 13M at 15 cm [6 in.]); f_y is yield strength; and f_u is ultimate strength.
1 cm = 0.394 in.; 1 cm = 10 mm; 1 MPa = 0.145 ksi.

Coarse aggregate in the concrete mixtures consisted of crushed limestone with a maximum size of 13 mm (0.5 in.). In specimen pairs S1 and S2, S3 and S4, and S7 and S8, concrete mixtures (with or without fibers) were obtained from a local ready mix concrete supplier. FRC (or fiber-reinforced mortar) in the other test specimens was mixed in the laboratory.

Mortar, as opposed to concrete, was used in the central region of Specimens S5 and S6, with proportions by weight of 1:0.4:1:0.15 for Type III cement, water, fly ash, and No. 16 silica sand. This sand has particles sized from mesh No. 20 (diameter of 0.85 mm [0.0335 in.]) to mesh No. 140 (diameter of 0.11 mm [0.00417 in.]). Mixture

proportions for the FRC used in Specimen S9 were 1:0.49:2.95:2.65 (Type III cement: water: coarse aggregate: 2NS sand), where 2NS sand refers to natural sand with particles sized from 10 mm (0.375 in.) to mesh No. 200 (diameter of 0.075 mm [0.00295 in.]), according to Section 902 of the 2003 Standard Specifications for Construction of the Michigan Department of Transportation (2003). Due to workability problems with this mixture, a different concrete mixture was used in Specimen S10 with the following proportions by weight: 1:0.48:1.45:1.55 (Type III cement: water: coarse aggregate: 2NS sand).

For Specimens S5, S6, S9, and S10, the FRC (or fiber-reinforced mortar) used in the slab central region and the regular concrete used elsewhere were cast nearly simultaneously. A methylmethacrylate formwork was placed in the central region of the slab to keep both materials separate while casting. Once the casting process was completed, the methylmethacrylate formwork was removed and modest vibration was applied to ensure adequate material transition between the central and outside portions of the slab. It should be mentioned that the concrete mixture used in Specimen S9 showed poor workability during casting, which led to significant air voids that had to be patched later.

Three 100 x 200 mm (4 x 8 in.) cylinders were prepared for each cement-based material (concrete or mortar) and tested for determination of average compressive strength within a week either before or after each slab test. Tests were conducted under displacement control. Cylinder strengths for each cement-based material are listed in Table 1.

Steel fibers

Three types of deformed steel fibers were used. Two of these fibers had hooks at their ends for mechanical anchorage, whereas the third type of fiber was twisted along its length. Geometrical and nominal material properties for these fibers are listed in Table 1.

Reinforcing steel

Reinforcing bars in all ten specimens were made of Grade 420M (Grade 60) steel. Steel reinforcement was ordered separately for each pair of specimens, except for Specimens S7 through S10, for which the steel came in a single shipment. For each steel bar shipment, five coupons were randomly selected for tensile testing. The average measured yield and ultimate strengths are listed in Table 1.

EXPERIMENTAL RESULTS

Observed damage

At the end of each test, the specimens were flipped over to mark cracks on the bottom (tension) side of the slab. In all tests, the column stub was clearly seen to punch through the slab; however, cracking on the slab bottom surface did not always give a clear indication that a punching shear failure had ultimately occurred. For instance, while the crack pattern on the slab bottom surface of Specimen S3 was typical of a punching shear failure (Fig. 3(a)), that observed in Specimen S6 was indicative of flexural yielding (Fig. 3(b)). In this case, it is believed that after initiation of the punching shear failure, the slab flexural reinforcement behaved as a "membrane" that was able to accommodate the large column stub vertical displacement and prevented the punching cone from surfacing at the bottom of the slab.

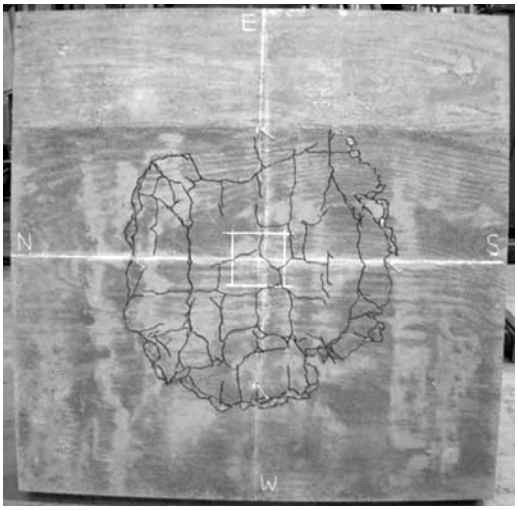

(a)

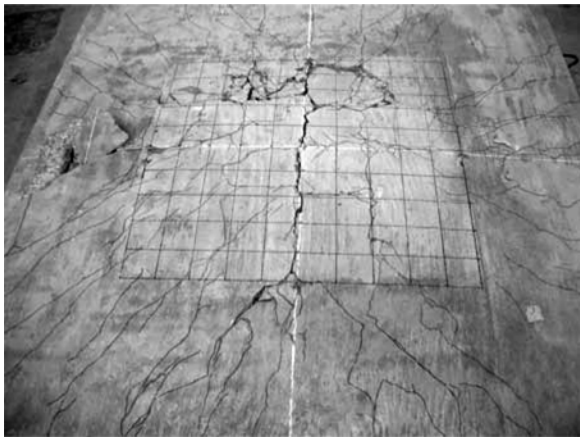

(b)

Fig. 3—Crack pattern on slab tension side: (a) Specimen S3; and (b) Specimen S6.

Load-versus-deflection response

Figure 4 shows the applied load P versus deflection response for the ten slab specimens. Two separate plots are provided: one corresponding to slabs with a flexural reinforcement ratio ρ in each principal direction of 0.83% (10 cm [4 in.] bar spacing), and the other to slabs with a reinforcement ratio of 0.56% (15 cm [6 in.] bar spacing). The flexural reinforcement ratio ρ was calculated as the area of a reinforcing bar divided by sh, where s is the bar spacing and h is the slab thickness.

In general, specimens with 10 cm (4 in.) reinforcing bar spacing showed greater initial stiffness and higher peak load compared with their counterpart specimens with 15 cm (6 in.) reinforcing bar spacing. Because failure in the specimens with 10 cm (4 in.) bar spacing occurred prior to or after limited flexural yielding, however, these specimens showed little or no ductility. On the other hand, flexural yielding preceded failure of the specimens with 15 cm (6 in.) reinforcing bar spacing, leading to increased ductility, particularly for Specimens S6 and S10 with a 1.5% volume fraction of twisted and high-strength hooked steel fibers, respectively.

Figure 5 shows the specimen responses in terms of the average punching shear stress ($P/b_o d$), normalized by the square root of the concrete cylinder strength f'_c, where b_o is

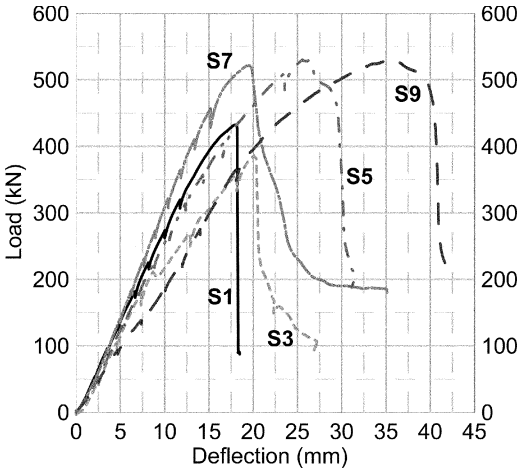

(a) Specimens with ρ = 0.83%

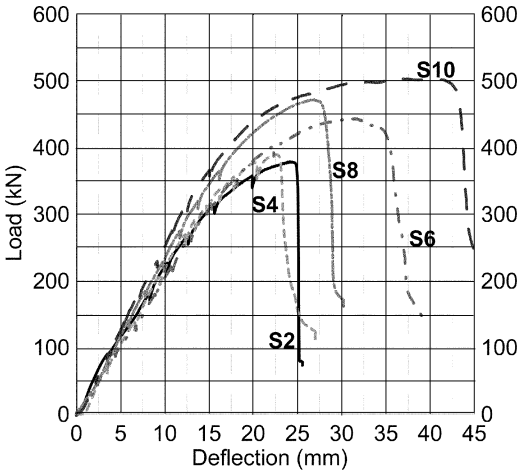

(b) Specimens with ρ = 0.56%

Fig. 4—Load-versus-deflection response. (Note: 1 kN = 0.225 kips; 1 mm = 0.0394 in.)

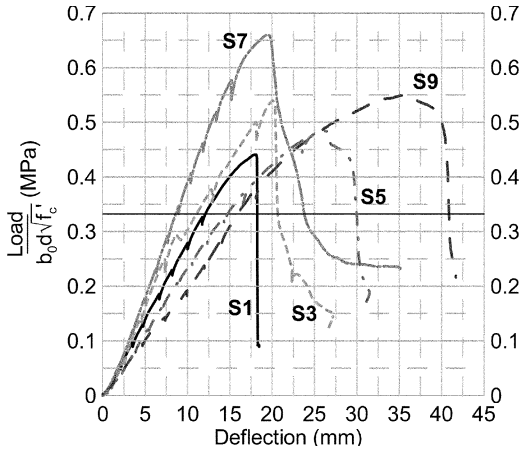

(a) Specimens with ρ = 0.83%

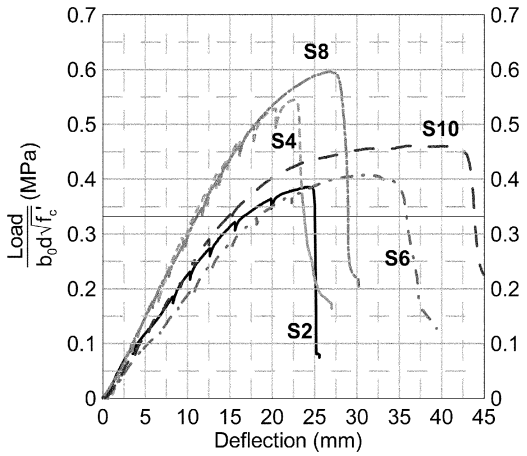

(b) Specimens with ρ = 0.56%

Fig. 5—Normalized shear stress versus deflection response. (Note: 1 MPa = 0.145 ksi; 1 mm = 0.0394 in.)

the critical perimeter and d is the slab effective depth. The perimeter b_o was calculated assuming the critical sections for shear to be located at $d/2$ from the faces of the support, according to the ACI Building Code (ACI Committee 318 2008). In the test specimens, the critical perimeter was equal to 112 cm (44 in.).

From Fig. 4 and 5, it is clear that the addition of fibers led to an increase in the normalized shear strength and/or ductility of the test specimens. The initial stiffness, however, was not affected by the presence of fibers, as expected. The lower stiffness exhibited by Specimen S9 (Fig. 4(a)) was believed to be due to air voids caused by poor concrete workability which, as mentioned previously, required patching prior to testing.

Measured peak loads and deflections at ultimate are summarized in Table 2. Also shown in Table 2 is the normalized shear strength, as defined in Fig. 5. It should be noted that all peak normalized strength values are greater than 1/3 (for f_c' in MPa), which is the ACI Code (ACI Committee 318 2008) strength factor applicable to the test slabs. Among all specimens, Specimens S7 and S8, reinforced with regular strength hooked steel fibers in a 1.5% volume fraction, displayed the largest normalized strength. Comparing the response of control Specimen S1 with that of Specimens S5 (twisted fibers) and S7 (regular strength hooked fibers), both with a 1.5% fiber volume fraction, an 11 and 50% increase in normalized shear strength was obtained, respectively. This suggests that, for the same fiber-volume ratio, these hooked steel fibers are more efficient than the twisted steel fibers in terms of normalized punching shear strength. Specimen S9 with high-strength hooked fibers in a 1.5% volume fraction, even though it required extensive patching prior to testing, showed a 25% higher normalized shear strength compared to control Specimen S1.

For the specimens with 15 cm (6 in.) bar spacing, strength comparisons are somewhat deceiving due to the fact that flexural yielding governed the strength of Specimens S6, S8, and S10. Specimen S10, reinforced with high-strength hooked steel fibers in a 1.5% volume ratio, exhibited the largest amount of flexural yielding (and ductility) prior to failing by punching. The results from the tests of Specimens S6, S8, and S10 are a clear indication that the increase in shear strength due to the presence of steel fibers in a 1.5% volume fraction allowed the slabs to develop their flexural strength prior to punching, with the associated increase in ductility. In practice, this increase in punching shear strength may translate into a change in failure mode from brittle punching shear to ductile flexural yielding.

Table 2—Summary of test results

Specimen	P_{max}, kN	$\frac{P_{max}}{b_o d\sqrt{f'_c}}$	δ_u, mm	$P_{yield\ line}$, kN	$\frac{P_{max}}{P_{yield\ line}}$	θ_u, rad
S1	433	0.44	18	539	0.80	0.013
S2	379	0.39	25	367	1.03	0.021
S3	386	0.54	20	494	0.78	0.013
S4	389	0.55	23	342	1.14	0.021
S5	530	0.49	30	545	0.97	0.018
S6	444	0.41	35	369	1.20	0.030
S7	522	0.66	20	499	1.05	0.015
S8	472	0.60	28	343	1.37	0.027
S9	530	0.55	40	514	1.03	0.027
S10	503	0.46	42	352	1.43	0.047

Notes: P_{max} is peak load; b_o is length of critical perimeter; d is slab effective depth; f'_c is in MPa; δ_u is deflection at failure; and θ_u is rotation at failure.
1 kN = 0.225 kips; 1 mm = 0.0394 in.; 1 MPa = 0.145 ksi.

One aspect that should be pointed out is that in specimen pairs S5 and S6, and S9 and S10, fibers were only added to the mixture used in the central 76 cm (30 in.) square region of the slab. The average shear stress calculated at the interface between the fiber-reinforced material and the regular concrete ranged between 0.18 and 0.22 $\sqrt{f'_c}$ (MPa) (2.2 and 2.6$\sqrt{f'_c}$ [psi]) for these four specimens. None of these specimens failed or exhibited distress at the interface between the FRC (or fiber-reinforced mortar) region and the surrounding regular concrete portion of the slab. These results indicate that the use of FRC can be restricted to the region where it is most needed, that is, the slab-column connection region. The limited test results suggest that a shear stress limit of (1/6) $\sqrt{f'_c}$ (MPa) (2 $\sqrt{f'_c}$ [psi]) could be used for estimating the location of the transition between FRC and concrete.

Yield-line analysis

The use of a yield-line analysis allows the estimation of the flexural capacity of RC slabs. The calculation of the flexural strength of the test specimens through yield-line analysis was performed following the yield-line pattern described by Elstner and Hognestad (1956) for slabs whose corners are free to lift by rotating about axis A-A in Fig. 6. The location of axis A-A (or distance x) is determined such as to minimize the resultant concentrated force. In the analyses, the measured yield strength of the reinforcing steel and the cylinder compressive strength of the concrete were used, while any contribution from the tensile resistance of FRC to moment strength was neglected. Typically, neither strain hardening of the steel reinforcement nor the effect of in-plane stresses is accounted for in yield-line analysis. Therefore, the result from a yield-line analysis is believed to represent a lower-bound estimation of the strength of the slab (assuming punching shear does not govern the slab strength).

Table 2 shows the experimental peak load and the load corresponding to the slab flexural capacity calculated from a yield-line analysis for each specimen. The load, normalized by the slab flexural capacity from the yield-line analysis, versus deflection response for the test specimens is presented in Fig. 7. The results from the yield-line analyses suggest that, except for Specimens S6, S8, and S10 (and likely Specimen S4), all specimens should have failed in punching shear with limited or no yielding of the reinforcing steel bars.

Criswell and Hawkins (1974) found that a slab ductile behavior was associated with values of ϕ_0 (peak load divided by strength estimated through yield-line analysis) between 1.1 and 1.2. Although specimens with ϕ_0 greater than 1.1 generally exhibited large deformations before punching failure, the test results suggest that $\phi \geq 1.2$ is more appropriate for ensuring substantial flexural yielding prior to punching shear failure in FRC slabs, as indicated by the behavior of Specimens S6, S8, and S10.

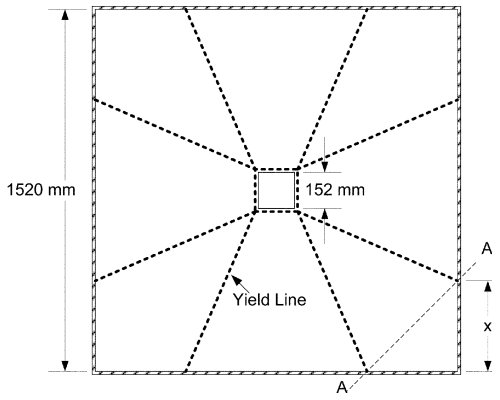

Fig. 6—Assumed yield-line pattern in test specimens (adapted from Elstner and Hognestad [1956]).

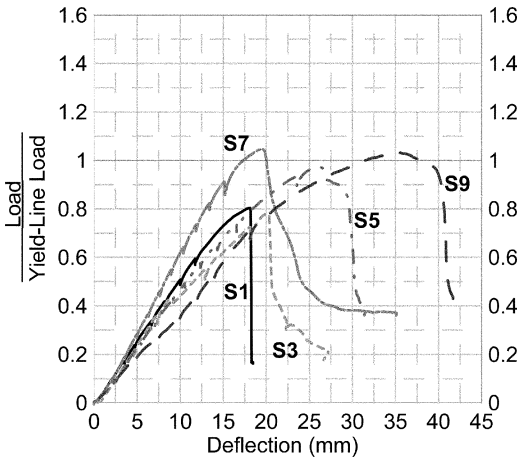

(a) Specimens with ρ = 0.83%

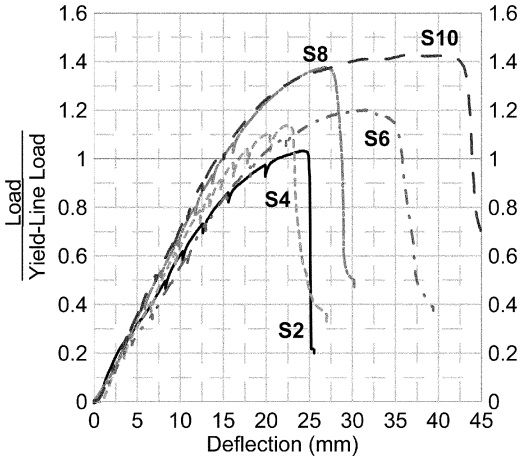

(b) Specimens with ρ = 0.56%

Fig. 7—Load (normalized by yield-line prediction) versus deflection response. (Note: 1 mm = 0.0394 in.)

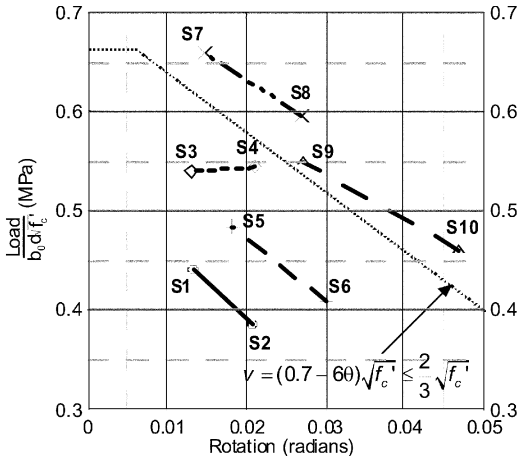

Fig. 8—Normalized shear stress-rotation interaction. (Note: 1 MPa = 0.145 ksi.)

Slab rotations

Slab rotations were measured over a distance of 305 mm (12 in.) from the column faces (twice the slab thickness). Average rotation values (from all four sides) at failure for all ten specimens are listed in Table 2, and a plot of the normalized shear strength versus average rotation at failure for all ten specimens is shown in Fig. 8. Failure in the test specimens was considered to have occurred when a sudden, major drop in the load occurred. In most specimens, this occurred at peak load.

Specimens with a reinforcement ratio equal to 0.56% (Specimens S2, S4, S6, S8, and S10) showed an average rotation capacity 1.7 times that of the specimens with a reinforcement ratio of 0.83% (Specimens S1, S3, S5, S7, and S9), while the peak normalized shear strength decreased, on average, by approximately 10%. The largest rotation ratio between each pair of specimens was 1.8 (Specimens S7 and S8), while the lowest ratio was 1.6 (Specimens S1 and S2). It is interesting to note that, except for Specimens S3 and S4, the slope for all specimen pairs was approximately the same and roughly represented a strength decay of $(1/16)\sqrt{f_c'}$ (MPa) per 0.01 rad rotation. The addition of fibers basically led to a translation of the response of the concrete specimens (Specimens S1 and S2) along either the load axis or the rotation axis, or both. Although the rate of strength decay could have been influenced by the difference in reinforcement ratio for each pair of slabs, this effect was believed to be minor for the reinforcement ratios considered (0.56 and 0.83%).

In Fig. 8, the closer points are to the upper right corner of the plot, the better the response is in terms of both punching shear strength and rotation capacity. Based on this criterion, the best responses corresponded to specimen pairs S7 and S8 with regular strength hooked steel fibers, and S9 and S10, with high-strength hooked steel fibers, all in a 1.5% volume fraction. For these four specimens, increases in punching shear strength and rotation capacity of up to approximately 55% and 125%, respectively, were obtained compared to the control specimens S1 and S2. Further, the shear stress v versus rotation θ points corresponding to these two pairs of specimens fall almost along a single line, which can be approximated as

$$v = (0.7 - 6\theta)\sqrt{f_c'} \le (2/3)\sqrt{f_c'} \quad \text{(MPa)} \qquad (1)$$

$$v = (8.4 - 72\theta)\sqrt{f_c'} \le 8\sqrt{f_c'} \quad \text{(psi)}$$

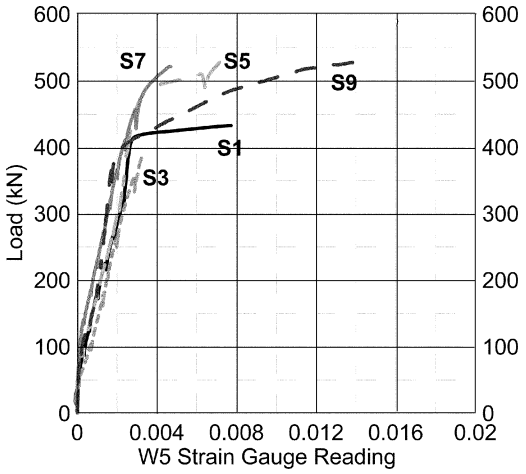

(a) Specimens with ρ = 0.83%

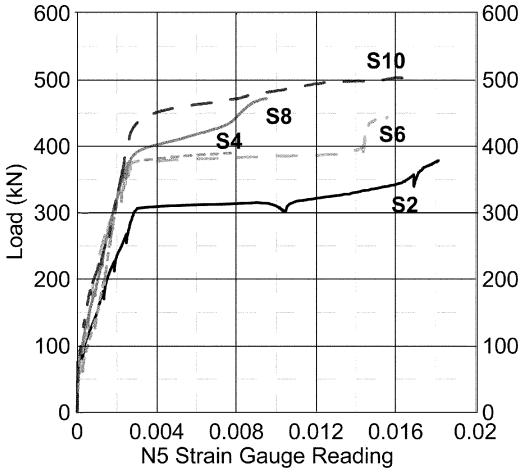

(b) Specimens with ρ = 0.56%

Fig. 9—Reinforcing bar strain history at d/2 from column stub face. (Note: 1 kN = 0.225 kips.)

The limited test results suggest, therefore, that for practical purposes, these two materials could be considered equally effective for improving slab punching shear resistance and/or deformation capacity.

Steel strains

Before discussing the strains measured in the test specimens, it is worth mentioning that strains in reinforcing bars embedded in FRC tend to be more sensitive to crack location than those in bars embedded in concrete. This is attributed to the enhanced bond between reinforcing bars and FRC. Thus, the reported strain readings should not be taken as a strict representation of the degree of inelastic deformation experienced by the slab reinforcing bars.

In all tests, strains were negligible prior to flexural cracking in the slab. Beyond cracking and prior to yielding, strains were basically proportional to the applied load. Readings from strain gauges located at *d*/2 from the column face indicate that some yielding occurred in the specimens with a reinforcement ratio of 0.83% prior to punching failure. Figure 9(a) shows the strain history at *d*/2 from the column stub face for one of the central slab bars (strain gauge W5 in Fig. 2(a)). Peak strains at this location ranged between 0.3% (Specimen S3) and

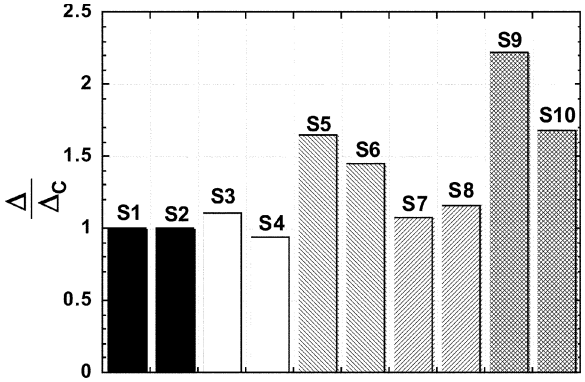

Fig. 10—Relative deflection capacity.

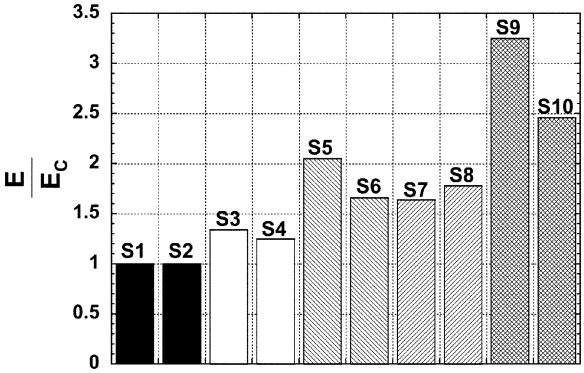

Fig. 11—Relative energy absorption capacity.

1.4% (Specimen S9). As expected, there was discrepancy in the strain gauge readings for the same specimen. Except for Specimen S9, the average peak strain at *d*/2 ranged between 0.4 and 0.6%. In Specimen S9, however, strains as large as 2% were measured at two locations and the average strain from all strain gauges at *d*/2 was 1.5%. At 1.5*d* away from the column faces, the measured strains at failure were at or below the yield point ($\varepsilon_y \cong 2.4 \times 10^{-3}$), except for Specimen S9, in which a peak tensile strain of 0.4% was measured.

For all specimens with a reinforcement ratio of 0.56%, peak strains at *d*/2 from the column face exceeded 1% in at least one bar. Specimens S2, S6, and S10 showed, on average, larger tensile strains with a peak strain of 2%. The strain history for one of the central bars in the slab specimens (strain gauge N5 in Fig. 2(b)) is shown in Fig. 9(b). At this location, peak strains of approximately 1.6% were measured in Specimens S2, S6, and S10, while peak strains of 1% and 0.8% were measured in Specimens S8 and S4, respectively. It is worth mentioning that although the strains measured in Specimen S2 were comparable to those in Specimens S6 and S10, the average rotation at failure for Specimen S2 was roughly 70% and 45% that of Specimens S6 and S10, respectively. These conflicting results could be attributed to the higher strain sensitivity to the crack location in bars embedded in FRC compared to that in bars embedded in concrete, as explained previously.

Reinforcement yielding in the specimens with a 0.56% reinforcement ratio spread to at least 1.5*d* from the column faces. Consistent with the strains measured at *d*/2 from the column face, the bars in Specimens S2, S6, and S10 exhibited the largest tensile strains, with values exceeding 1% in several bars.

Influence of fiber reinforcement on deflection capacity

The ability of fiber reinforcement to increase the deflection capacity of the test specimens was evaluated through the ratio Δ/Δ_C. The variable Δ_C refers to the deflection of either Specimen S1 or Specimen S2 at failure for specimens with flexural reinforcement ratio of 0.83% and 0.56%, respectively. The variable Δ, on the other hand, is the deflection at failure for each test specimen. A plot of Δ/Δ_C for all ten test specimens is shown in Fig. 10. As can be seen, among all test slabs, Specimens S9 and S10 exhibited the best performance with an increase of approximately 120% and 70% in deflection capacity compared to control Specimens S1 and S2, respectively.

Energy absorption

Energy absorption capacity of the test specimens was evaluated based on the area under the normalized punching shear stress versus deflection response. For each FRC specimen, the calculated energy E was normalized by that of the corresponding control specimen, E_C (Specimens S1 and S2 for slabs with 0.83% and 0.56% reinforcement ratio, respectively).

Figure 11 shows the calculated values of normalized energy absorbed. As can be seen, the addition of fibers to the concrete led to an increase in energy absorption, particularly in the specimens with 1.5% fiber volume fraction (Specimens S5 through S10). For the same fiber-volume ratio (1.5%), the specimens reinforced with either twisted fibers or regular strength hooked steel fibers absorbed comparable amounts of energy. Specimens S5 and S6 with twisted fibers exhibited a larger displacement at failure, while Specimens S7 and S8 with regular strength hooked fibers showed a higher normalized shear strength. Specimens S9 and S10 with high-strength hooked steel fibers exhibited the largest energy absorption capacity. These two specimens showed moderate peak strengths but superior deformation capacity.

SUMMARY AND CONCLUSIONS

Ten slab specimens, eight of them constructed with steel FRC (or fiber-reinforced mortar), were tested under monotonically increased concentrated load. Three different types of steel fibers were evaluated, that is, regular strength (1100 MPa [160 ksi]) hooked fibers, high-strength (2300 MPa [334 ksi]) hooked fibers, and twisted fibers (1800 MPa [260 ksi]) in a ratio of either 1 or 1.5% by volume. From the results presented, the following conclusions can be drawn.

1. The addition of fibers led to an increase in slab punching shear strength and/or deformation capacity. Of all test slabs, the specimens with either regular strength or high-strength hooked steel fibers in a 1.5% volume fraction exhibited the best behavior in terms of shear strength-rotation interaction, with increases in punching shear strength and rotation capacity of up to approximately 55% and 125%, respectively. No appreciable change in stiffness was observed due to the addition of fibers.

2. The increase in punching shear strength due to the use of FRC may lead to a change in failure mode from punching shear failure to flexural yielding. The behavior of the slab specimen with 1.5% volume fraction of high-strength hooked steel fibers and a 0.56% flexural reinforcement ratio in each principal direction (Specimen S10) partially illustrated this

phenomenon. In this specimen, the increase in punching shear resistance allowed the slabs to exhibit substantial flexural yielding before a punching shear failure ultimately occurred.

3. Test results showed that FRC only in the connection region over two slab thicknesses from each column stub face was sufficient to increase punching shear resistance in the test specimens. A limit of (1/6) $\sqrt{f'_c}$ (MPa) (2 $\sqrt{f'_c}$ [psi]) for the average shear stress outside of the FRC region was found to be adequate for determining the extension of the FRC portion of the slab.

ACKNOWLEDGMENTS

This research was sponsored by the U.S. National Science Foundation, as part of the Network for Earthquake Engineering Simulation (NEES) Program, under Grant No. CMS 0421180. The opinions expressed in this paper are those of the writers and do not necessarily express the views of the sponsor.

REFERENCES

ACI Committee 318, 2008, "Building Code Requirements for Structural Concrete (ACI 318-08) and Commentary," American Concrete Institute, Farmington Hills, MI, 473 pp.

Alexander, S. D. B., and Simmonds, S. H., 1992, "Punching Shear Tests of Concrete Slab-Column Joints Containing Fiber Reinforcement," *ACI Structural Journal*, V. 89, No. 4, July-Aug., pp. 425-432.

Cheng, M.-Y., and Parra-Montesinos, G. J., 2009, "Punching Shear Strength and Deformation Capacity of Fiber Reinforced Slab-Column Connections under Earthquake-Type Loading," *Report* UMCEE 09-01, Department of Civil and Environmental Engineering, University of Michigan, Ann Arbor, MI, 334 pp.

Cheng, M.-Y., and Parra-Montesinos, G. J., 2010, "Steel Fiber Reinforcement for Punching Shear Resistance in Slab-Column Connections—Part II: Lateral Displacement Reversals," *ACI Structural Journal*, V. 107, No. 1, Jan.-Feb., pp. 110-118.

Corley, W. G., and Hawkins, N. M., 1968, "Shear Head Reinforcement for Slabs," ACI JOURNAL, *Proceedings* V. 65, No. 10, Oct., pp. 811-824.

Criswell, M. E., and Hawkins, N. W., 1974, "Shear Strength of Slabs: Basic Principle and Their Relation to Current Methods of Analysis," *Shear in Reinforced Concrete*, SP-42, American Concrete Institute, Farmington Hills, MI, pp. 641-676.

Dilger, W. H., and Ghali, A., 1981, "Shear Reinforcement for Concrete Slabs," *Journal of the Structural Division*, ASCE, V. 107, No. ST12, pp. 2403-2420.

Elstner, R. C., and Hognestad, E., 1956, "Shearing Strength of Reinforced Concrete Slabs," ACI JOURNAL, *Proceedings* V. 53, No. 1, Jan., pp. 29-58.

Harajli, M. H.; Maalouf, D.; and Khatib, H., 1995, "Effect of Fibers on the Punching Shear Strength of Slab-Column Connections," *Cement and Concrete Composites*, V. 17, No. 2, pp. 161-170.

Hawkins, N. M.; Mitchell, D.; and Sheu, M. S., 1974, "Cyclic Behavior of Six Reinforced Concrete Slab-Column Specimens Transferring Moment and Shear," *Progress Report* 1973-74 on NSF Project GI-38717, Department of Civil Engineering, University of Washington, Seattle, WA, Sept.

Islam, S., and Park, R., 1976, "Tests of Slab-Column Connections with Shear and Unbalanced Flexure," *Journal of the Structural Division*, ASCE, V. 102, No. ST3, pp. 549-569.

McHarg, P. J.; Cook, W. D.; Mitchell, D.; and Yoon, Y.-S., 2000, "Benefits of Concentrated Slab Reinforcement and Steel Fibers on Performance of Slab-Column Connections," *ACI Structural Journal*, V. 97, No. 2, Mar.-Apr., pp. 225-234.

Michigan Department of Transportation (MDOT), 2003, "Standard Specifications for Construction," http://mdotwas1.mdot.state.mi.us/public/specbook/, accessed on January 12, 2009.

Naaman, A. E.; Likhitruangsilo, V.; and Parra-Montesinos, G., 2007, "Punching Shear Response of High-Performance Fiber-Reinforced Cementitious Composite Slabs," *ACI Structural Journal*, V. 104, No. 2, Mar.-Apr., pp. 170-179.

Shaaban, A. M., and Gesund, H., 1994, "Punching Shear Strength of Steel Fiber-Reinforced Concrete Flat Plates," *ACI Structural Journal*, V. 91, No. 4, July-Aug., pp. 406-414.

Swamy, R. N., and Ali, S. A. R., 1982, "Punching Shear Behavior of Reinforced Slab-Column Connections Made with Steel Fiber Concrete," ACI JOURNAL, *Proceedings* V. 79, No. 5, May, pp. 392-406.